Aerosol and Air Quality Research, 14: 1573–1583, 2014

ISSN: 1680-8584 print / 2071-1409 online
doi: 10.4209/aaqr.2013.04.0119

Effect of the Quartz Particle Size on XRD Quantifications and Its Implications for Field Collected Samples

Ching-Hwa Chen[1], Jhy-Charm Soo[2], Li-Hao Young[2], Trong-Nen Wu[2], Chungsik Yoon[3], Chane-Yu Lai[4], Perng-Jy Tsai[1,2*]

[1] Department of Environmental and Occupational Health, Medical College, National Cheng Kung University, 138, Sheng-Li Rd., Tainan 70428, Taiwan
[2] Department of Occupational Safety and Health, College of Public Health, China Medical University and Hospital, 91, Hsueh-Shih Rd, Taichung 40402, Taiwan
[3] Institute of Health and Environment, School of Public Health, Seoul National University, 1 Gwanak-ro, Gwanak-gu, Seoul 151-742, Korea
[4] Department of Occupational Medicine, Chung Shan Medical University Hospital, 110, Sec.1, Jianguo N. Rd., Taichung City 40201, Taiwan

ABSTRACT

The aims of the present study were to assess the effect of the quartz particle size on XRD quantifications, and use it to develop models for correcting the measured quartz concentrations of samples collected from the field. Seven nearly mono-dispersed pure quartz dusts, with mass median aerodynamic diameters (MMAD) ranging from 0.70 to 10.84 μm, were prepared by a liquid sedimentation device, and their unit XRD intensities (UI) were measured using the NIOSH Method 7500. The results show that UI increases (from 063 to 1.14) along with the rise in MMAD of the pure quartz dust. To examine the impact of the above results on quantifying field collected samples, both total dust and respirable dust samplings were conducted at seven different workplace environments. The results show that the quartz particles contained in all collected total dust samples (MMAD = 5.18–16.7 μm, GSD = 2.08–2.88) were coarser in their particle sizes than that of the reference quartz standard (NIST-SRM 1878; MMAD = 2.16 μm, GSD = 1.55), and the measured total quartz particle concentrations (C_m) were 16.6–22.5% lower than the corresponding true concentrations (C_t). However, for respirable dust samples (MMAD = 1.37–3.95 μm, GSD = 1.978–2.87), since collected quartz particle sizes could be either finer or coarser than that of the reference standard, both underestimation and overestimation were found in the present study (C_m/C_t = 0.881–1.09). To correct the measured concentrations of field collected samples, correcting models were developed based on the MMADs of the collected quartz particle samples and their corresponding UIs. This study yields correcting factors for the respirable fraction (CR_f) as $CR_f = 1.50 - 0.67 \times [1 - \exp(-0.69 \times \text{MMAD})]$ ($R^2 = 0.996$, n = 7). However, the obtained CR_f should be used with caution if the collected samples were found with quartz particle sizes falling outside the size range of the present study.

Keywords: Quartz; Particle size distribution; X-ray diffraction; Exposure assessment.

INTRODUCTION

To date, both the NIOSH 7500 X-ray diffraction (XRD) method (NIOSH, 2003) and the NIOSH 7602 infrared (IR) spectrophotometer method (NIOSH, 1994) have been widely used for quantifying collected free crystalline silica (including quartz, tridymite, and cristobalite) filter samples. In principle, the former is considered to be better than the latter due to its higher precision and accuracy (William, 1999). However, the accuracy associated with using XRD in quantification could be affected by the particle size of the crystalline silica containing in the collected sample. Many researchers have found that the measured XRD intensities increase with the increase in quartz particle sizes (Bhaskar *et al.*, 1994; Yabuta and Ohta, 2003). However, it should be noted that the metrics used for describing the quartz particle size in the above studies were inconsistent. For example, the equivalent volume diameter (d_v) was used by Bhaskar *et al.* (1994), and the aerodynamic diameter (d_{ae}) was adopted by Yabuta and Ohta (2003). Therefore,

* Corresponding author.
Tel.: +886-4-2353535 ext. 5806; Fax: +886-6-2752484
E-mail address: pjtsai@mail.ncku.edu.tw

developing a detailed numerical model for describing the relationship between the measured XRD intensities and the corresponding quartz particle sizes, by using the metric related to human exposure, would be of importance to the environmental health science field for conducting exposure assessments. In addition, it is known that particle sizes of a free crystalline silica reference standard used for XRD quantifications are poly-dispersed, and would have intrinsic differences in particle size distribution from those field collected samples. Therefore, it can be expected that quartz particle samples with various size distributions, though their true concentration are the same, would result in different measured concentrations even the same reference standard was used in the XRD analysis process (Kauffer *et al.*, 2002; Chisholm, 2005; Stacey *et al.*, 2009). To date, the effect associated the use of a reference standard on the quantification of field collected samples has never been assessed. In addition, the establishment of a suitable method for converting the measured concentration to true concentration would be of importance for conducting exposure assessment.

The first aim of this study is set out to numerically assess the effect associated with the particle size of crystalline silica on its measured XRD intensity. For illustration, only quartz was studied in the present study because it is the one most encountered in the environmental health science field among all crystalline silica types (Shih *et al.*, 2008). The metric of the aerodynamic diameter (d_{ae}), which has been recognized as the one most related to human exposure to micrometer particles, was adopted in the present study (Vincent, 2007). To date, the NIST-SRM 1878 (MMAD = 2.16 μm, GSD = 1.55; National Institute of Standards and Technology, Gaithersburg, USA), as recommended by Verma and Shaw (Verma and Shaw, 2001), has been widely used as the reference standard for quartz quantifications. Therefore, the effect associated the use of it on quantifying field collected quartz samples was also investigated. Finally, nonlinear regression models were developed to correct the quantitative results for field collected samples while the NIST-SRM 1878 was used as the reference standard. The results obtained from the present study would be beneficial to the environmental health science field for accurately evaluating human quartz exposures.

MATERIALS AND METHODS

Preparation of Pure Quartz Dust with Various Particle Sizes

The quartz dust with a purity of ~99.0% and equivalent volume diameter (d_v) of ~15.1 μm ($d_{v90\%}$ = ~39 μm) (Pei Long Enterprise Co., Ltd., Changhua, Taiwan) was used for preparing pure quartz dust samples with various quartz particle sizes. The quartz dust was pretreated with phosphoric acid for 2 hr to remove metal impurities. Metals containing in pretreated quartz dust were analyzed per the NIOSH 7300 method using inductively coupled plasma-atomic emission spectroscopy (ICP-AES, JY 2000, HORIBA Jobin Yvon, Longjumeau, France). A total of 22 metal elements were analyzed with the method of detection limits (MDLs) ranging from 2.01×10^{-3} to 10.7×10^{-3} mg.

To separate quartz dust into various particle sizes in d_{ae}, a 10 g of pretreated pure quartz dust was placed into a liquid sedimentation device (Fig. 1). Before the separation process, distilled water was added into the device until the water level reached 10 cm, and then ultrasonic shaking was conducted for 10 min to keep the pretreated pure quartz dust suspending in the water. The separation of particles was conducted via several repeated sedimentation processes with various specified settling times (t), which were determined according to Stokes' law. The equation for the determination

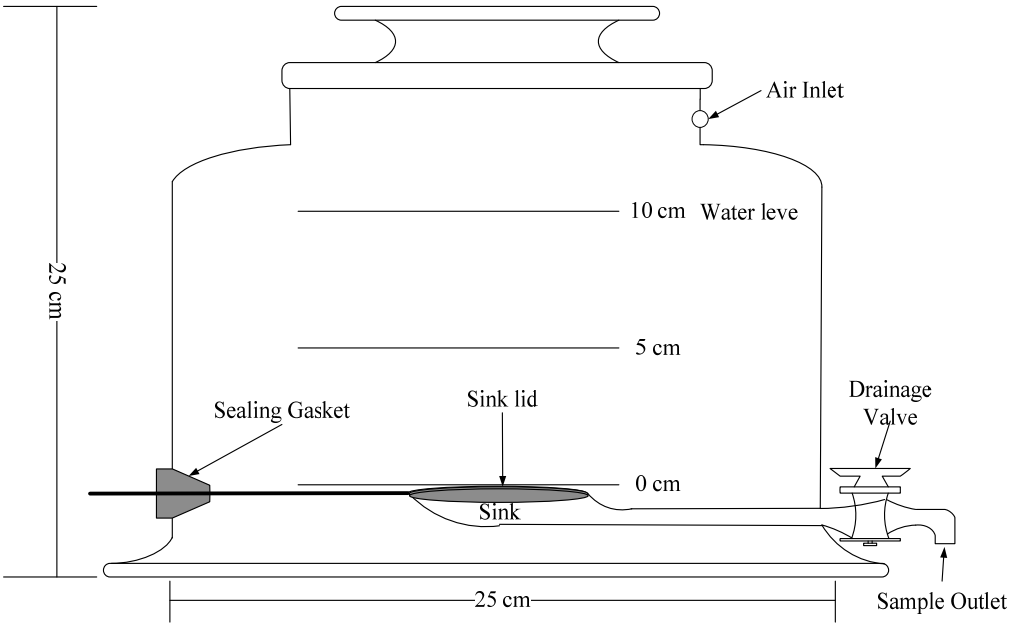

Fig. 1. The schematic of the liquid sedimentation device used in the present study.

of the t (sec) can be expressed as the following:

$$t = \left[\frac{18 \times \eta \times 10^8}{\left(\rho_p - \rho_0\right) \times G \times (d'_{ae})^2} \right] \times L \quad (1)$$

where η is the viscosity coefficient of the medium (i.e., water) at 20°C (= 1.01 × 10^{-2} g/cm·s), ρ_p is the density of the quartz dust (= 2.65 g/cm^3), ρ_0 is the density of water (= 0.998 g/cm^3 at 20°C), G is the gravitational acceleration (= 980 cm/s^2), d'_{ae} is the targeted particle size to be separated in aerodynamic diameter, and L is the settling distance for the pure quartz dust (= height of the water level of the device = 10 cm). This study yielded t specified for quartz dust with d'_{ae} values of 0.8, 1.2, 2.0, 3.0, 6.0, 9.0, and 12.0 μm were 48 hr 44 min, 21 hr 39 min, 7 hr 47 min, 3 hr 27 min, 52 min, 23 min 6s, and 13 min, respectively.

The particle size separation process began with a settling time of 48 hr 44 min. During the sedimentation process, the sink lid was place on the sink top to prevent from the error associated with the deposition of pretreated pure quartz dusts directly onto the sink. After the first sedimentation process, the water suspension was collected by removing the sink lid from the sink top and opening the drainage valve simultaneously. The collected water was filtrated by a mixed cellulose ester (MCE) filter with a 0.8-μm pore size. The filter was then placed in a furnace for 2 hr at 600°C to obtain the separated pure quartz dust with d'_{ae} < 0.8 μm. The same process was repeated for the other six designated settling times in order to separate pure quartz dust with d'_{ae} of 0.8–1.2, 1.2–2.0, 2.0–3.0, 3.0–6.0, 6.0–9.0, and 9.0–12.0 μm, respectively. A similar device has been used in one study conducted for the same purpose (Yabuta and Ohta, 2003).

Determining the True Particle Sizes of the Separated Pure Quartz Dust

Separated pure quartz dusts with d'_{ae} of < 0.8, 0.8–1.2, 1.2–2.0, 2.0–3.0, and 3.0–6.0 μm were further measured using a transmission electron microscope (TEM, JEM-1400, JEOL Co., Ltd, Tokyo, Japan) to determine their projected area diameters (d_p; μm). For those separated pure quartz dusts with d'_{ae} of 6.0–9.0, and 9.0–12.0 μm, their d_p were determined using a scanning electron microscope (SEM, S4100, Hitachi, Tokyo, Japan). Here, 0.01 mg of each separated pure quartz dust was first mixed with 5 mL of distilled water and then had a ultrasonic shaking for 10 min. For TEM analyses, 10 μL of suspension was placed on a slide and dried. For SEM observations, 10 μL of suspension was placed on a conductive carbon tape, dried, and gilded. For each separated pure quartz dust, ~15 TEM (or SEM) images were obtained. ~100 particles were measured and their d_p values were were used to determine the true aerodynamic diameter (d''_{ae}; μm) using equation of the following:

$$d''_{ae} = \frac{d_p}{S_v \times \left(\frac{\rho_0 S_D}{\rho_p} \right)} \quad (2)$$

where S_D is the dynamic shape factor of the pure quartz dust (= 1.36) and S_v is the volume shape factor of quartz (= 1.25) (Davies, 1979). The obtained d''_{ae} values were used to determine the number-based particle size distribution (including the number median aerodynamic diameter (NMAD) and the geometric standard deviation (GSD)) of the separated pure quartz dust. For any given particle size distribution, it is known that both of its number-based and mass-based size distribution share the same GSD (Baron and Willeke, 2001). According to the Hatch-Choate equation, the mass median aerodynamic diameter (MMAD) can be determined by the following (Vincent, 1995):

$$\text{MMAD} = \text{NMAD} \times \exp(3 \times \ln^2 \text{GSD}) \quad (3)$$

XRD Analyses of the Separated Pure Quartz Dusts

The unit XRD intensity (UI, XRD intensity/μg) for each separated pure quartz dust was determined per NIOSH Method 7500 through XRD analysis (NIOSH, 2003). For XRD analysis, scanning was performed in a 2θ range of 15° to 65°. The scanning speed was 1°/min and the step size was 0.01°. The calibration curve for all separated pure quartz dusts covered the range of 25 to 1000 μg with R^2 of ~0.998. By analyzing three samples for each separated pure quartz dust with a given concentration, the accuracy and precision were found to be ~3.3% and ~4.0%, respectively. By analyzing 7 samples on different days, the instrument stability was found to be ~10%. This study yielded a MDL of ~0.024 mg from all separated pure quartz dusts for quantifying their quartz content.

In the present study, a nonlinear regression equation was used to describe the relationship between UI and its corresponding d''_{ae}, and the effect associated with the quartz particle size on XRD quantification was assessed.

Field Sampling and Sample Analyses

In this study, field samplings were conducted at three sampling workplaces in an iron and steel plant (including the air stove, coke oven/roof, and coke oven/sidewalk) during the stove repairing period, and four work stages inside a municipal waste incinerator during its annual maintenance period (including the stove repairing, refractory material repairing, scaffold removing, and stove cleaning).

For each selected workplace (or work stage), three cascade impactors (Marple 298 cascade impactor, Thermo Andersen Inc., Smyrna, GA, USA) were used for conducting particle-size-segregating samplings with a sampling flow rate specified at 2.0 L/min. The cascade impactor consists of eight impaction stages ($d_{ae50\%}$ = 0.52, 0.96, 1.55, 3.5, 6.0, 9.8, 14.8, and 21.3 μm, respectively) and a back-up filter (34-mm PVC filter with 5.0-μm pore size; Omega Specialty Instrument, Co., Houston, USA). For sample collected on the i^{th} impaction stage, its measured XRD intensity (I_i) was determined per NIOSH Method 7500 as described in the previous section (NIOSH, 2003).

Determining True Quartz Concentrations for Field Collected Samples

For sample collected on the i^{th} impaction stage, its true

quartz concentration (C_{ti}) could be determined by its measured XRD intensity (I_i) and the corresponding unit intensities (UI_{ci}). Here, UI_{ci} can be calculated based on $d_{ae50\%}$ of the i^{th} impaction stage and the nonlinear regression equation, which was used to describe the relationship between UI and its corresponding d''_{ae} (see section 2.3). The true quartz concentration (C_{ti}) could then be determined by the following:

$$C_{ti} = \frac{I_i}{UI_{ci}} \tag{4}$$

The resultant C_{ti} of the eight impaction stages were used to describe the true particle size distribution of the quartz content found in the workplace atmosphere. In addition, by summing up the concentrations of the eight impaction stages and the result was regarded as the total true quartz concentrations (C_t; the concentration of all quartz particles containing in the atmosphere of the selected workplace). Here, C_t can be determined by the following:

$$C_t = \sum_{i=1}^{8} C_{ti} = \sum_{i=1}^{8} \frac{I_i}{UI_{ci}} \tag{5}$$

In this study, the concentration of the respirable fraction (CR_i) for sample collected on the i^{th} impaction stage can be obtained by the collected concentration (C_{ti}) and the corresponding respirable fraction (R_i) of dusts collected on the stage. Here, R_i can be obtained from the criteria currently adopted by the International Standards Organization (ISO), Comité Européen Normalization (CEN), and American Conference for Governmental Industrial Hygienists (ACGIH) (ACGIH, 1995–1996; CEN, 1992; ISO; 1992). In this study, CR_i can be determined by the following:

$$CR_i = C_{ti} \times R_i \tag{6}$$

Again, the resultant CR_i of the eight stages were used to describe the particle size distribution of the respirable quartz content found in the workplace atmosphere. Through the integration of the respirable fraction of the eight impaction stages, the true respirable quartz concentration (CR_t) can then be determined by the following:

$$CR_t = \sum_{i=1}^{8} CR_i = \sum_{i=1}^{8} C_{ti} \times R_i = \sum_{i=1}^{8} \frac{I_i}{UI_{fi}} \times R_i \tag{7}$$

Determining Measured Quartz Concentrations and Their Corresponding Conversion Factors for Field Collected Samples

To date, the NIST-SRM 1878 has been widely used as the reference standard for the quantification of field collected quartz samples. In this study, the unit intensity for NIST-SRM 1878 (UI_{NIST}, XRD intensity/μg) was also determined per NIOSH Method 7500 through XRD analysis (NIOSH, 2003). This study yielded UI_{NIST} as 0.840 XRD intensity/μg. By reference to the standard of NIST-SRM 1878, the measured quartz concentration for sample collected on the i^{th} impaction stage (C_{mi}) can be determined by the following:

$$C_{mi} = \frac{I_i}{UI_{NIST}} \tag{8}$$

The total measured quartz concentrations (C_m) can be determined by adding up the concentrations of the eight impaction stages as the following:

$$C_m = \sum_{i=1}^{8} C_{mi} = \sum_{i=1}^{8} \frac{I_i}{UI_{NIST}} \tag{9}$$

In the present study, the conversion factor (C_f) was defined as the following:

$$C_f = \frac{C_t}{C_m} \tag{10}$$

In principle, if C_f could be obtained for samples collected from a given size distributions, it would be useful for converting C_m into C_t in the field. In this study, a nonlinear regression model was developed for describing C_f and samples with various size distributions for the above purpose.

By taking the respirable fraction into account, the measured respirable quartz concentration for sample collected on the i^{th} impaction stage (CR_{mi}) can be determined by the following:

$$CR_{mi} = C_m \times R_i \tag{11}$$

Using the CR_{mi} of the eight impaction stages, the particle size distribution of the respirable quartz can be determined (in terms of its MMAD and GSD). Finally, the summation of CR_{mi} of the eight impaction stages is calculated as the total measured respirable quartz concentration (CR_m) by the following:

$$CR_m = \sum_{i=1}^{8} CR_{mi} = \sum_{i=1}^{8} C_{mi} \times R_i = \sum_{i=1}^{8} \frac{I_i}{UI_{NIST}} \times R_i \tag{12}$$

Again, the conversion factor for the respirable fraction (CR_f) was defined as the following:

$$CR_f = \frac{CR_t}{CR_m} \tag{13}$$

For converting CR_m into CR_t in the field, a nonlinear regression model was developed in the present study for describing C_f and samples with various size distributions.

RESULTS AND DISCUSSION

Separated Pure Quartz Dusts

Table 1 shows metal contents found in pure quartz dusts after being pretreated with phosphoric acid. Among 22 analyzed metal elements, only 7 (Cd, Co, Cr, Cu, Ni, Pb, and

Table 1. Metal contents containing in the pretreated pure quartz dust (n = 3).

Metal	Mean ± SD (%, by weight)
Cd	$5.10 \times 10^{-3} \pm 3.20 \times 10^{-3}$
Co	$9.10 \times 10^{-3} \pm 6.20 \times 10^{-3}$
Cr	$1.40 \times 10^{-2} \pm 5.10 \times 10^{3}$
Cu	$2.10 \times 10^{-2} \pm 2.20 \times 10^{-2}$
Ni	$4.60 \times 10^{-3} \pm 4.00 \times 10^{-3}$
Pb	$8.70 \times 10^{-2} \pm 3.30 \times 10^{-2}$
Ti	$7.00 \times 10^{-1} \pm 7.9 \times 10^{-2}$
Total	$8.40 \times 10^{-1} \pm 6.3 \times 10^{-2}$

Ti) were detectable and in total accounted only for ~0.84% of the weight. In the present study, ~10 g of pretreated pure quartz dust was put into a liquid sedimentation device (Fig. 1) in order to classify it into various targeted particle sizes (d'_{ae}).

The images for those separated pure quartz dust with d'_{ae} < 0.8, 0.8–1.2, 1.2–2.0, 2.0–3.0, and 3.0–6.0 μm were measured using a TEM (JEM-1400, JEOL Co., Ltd, Tokyo, Japan) to determine their projected area diameters (d_p). For those with d'_{ae} of 6.0–9.0 and 9.0–12.0 μm, their d_p were determined according to images measured by an SEM (S4100, Hitachi, Tokyo, Japan). For illustration, Fig. 2 shows the images of separated pure quartz dusts with d'_{ae} of 2–3 μm and 6–9 μm obtained from TEM and SEM, respectively. In this study, the true particle size (d''_{ae}) for each separated pure quartz dust was determined by applying the corresponding d_p obtained from TEM (or SEM) images to Eq. (2). The resultant d''_{ae} values were used to determine the number-based particle size distribution (including the number median aerodynamic diameter (NMAD) and the geometric standard deviation (GSD)). Since both number-based and mass-based size distribution share the same GSD, the Hatch-Choate equation was used to convert NMAD to the mass median aerodynamic diameter (MMAD) according to Eq. (3). Table 2 shows the resultant true particle size distribution (shown as its MMAD ± GSD) of d''_{ae} for each separated pure quartz dust. Here, d'_{ae} of < 0.8, 0.8–1.2, 1.2–2.0, 2.0–3.0, 3.0–6.0, 6.0–9.0, and 9.0–12.0 μm were found with d''_{ae} of 0.700 μm ± 1.66, 1.05 μm ± 1.81, 1.94 μm ± 1.53, 2.76 μm ± 1.55, 5.25 μm ± 1.44, 8.51 μm ± 1.39, and 10.9 μm ± 1.50, respectively. All resultant GSD were found around 1.50 indicating that each separated pure quartz dust was quite mono-dispersed. Therefore, the MMAD was considered adequately to characterize the particle size for each separated pure quartz dust.

Effect of Quartz Particle Size on Measured XRD Intensities

Table 2 also shows the obtained UI (XRD intensity/μg) for each separated pure quartz dust. Fig. 3 shows the relationship between UI and MMAD obtained from the seven separated pure quartz dust samples. This study yielded a nonlinear regression equation for the above relationship as:

$$\text{UI (MMAD)} = 0.498 + 0.681[1 - \exp(-0.318 + \text{MMAD})] \quad (R^2 = 0.996,\ n = 7) \tag{14}$$

Obviously, our results suggest that the value of UI is increased as the increase in MMAD. The above trend is consistent with those reported by previous research works (Bhaska *et al.*, 1994; Yabuta and Ohta, 2003). In addition, the results also indicate that UI values are increased sharply for those *MMAD* from 0.700 to 5.25 μm, but slowly for those from 5.25 to 10.8 μm. Here, it should be noted that the UI for MMAD of 0.700 μm (i.e., 0.63 ± 0.08 XRD intensity/μg) is only ~0.553 times in magnitude as that of 10.84 μm (i.e., 1.14 ± 0.02 XRD intensity/μg). Therefore, if quartz dust samples with the above two MMAD were found with the same XRD intensity, the quantification result for the former would be ~1.81 times in magnitude higher than that of the latter. The above result further indicates the significant effect of the quartz particle size on XRD quantification results.

True Quartz Concentrations and Their Conversion Factors for the Field Collected Samples

Table 3 shows the unit intensities (UI_{ci}) for samples collected on the i^{th} impaction stages of the cascade impactor used in the present study. Here, UI_{ci} was calculated based on $d_{ae50\%}$ of the i^{th} impaction stage and the obtained nonlinear regression model (see Eq. (14)). For each selected

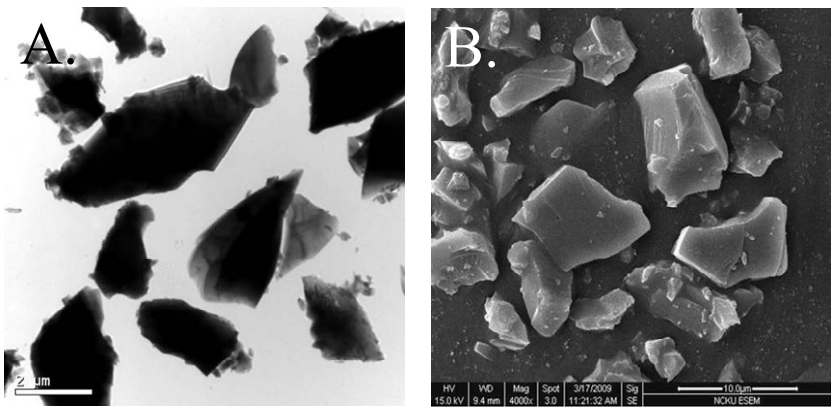

Fig. 2. Projected areas of separated pure quartz particles obtained from (A) TEM (for d'_{ae} = 2–3 μm), and (B) SEM (for d'_{ae} = 6–9 μm).

Table 2. Targeted particle sizes (d'_{ae}), their corresponding true particle sizes (d''_{ae}) and mean unit intensities (UI) of the seven separated pure quartz dusts.

Targeted particle sizes (d'_{ae}; μm)	True particle size (d''_{ae}; μm)	UI (XRD intensity/μg)
	MMAD ± GSD	Mean ± SD
< 0.8	0.700 ± 1.66	0.63 ± 0.08
0.8–1.2	1.05 ± 1.81	0.68 ± 0.02
1.2–2.0	1.94 ± 1.53	0.80 ± 0.03
2.0–3.0	2.76 ± 1.55	0.88 ± 0.02
3.0–6.0	5.25 ± 1.44	1.07 ± 0.04
5.0–9.0	8.51 ± 1.39	1.12 ± 0.03
9.0–12.0	10.84 ± 1.50	1.14 ± 0.02

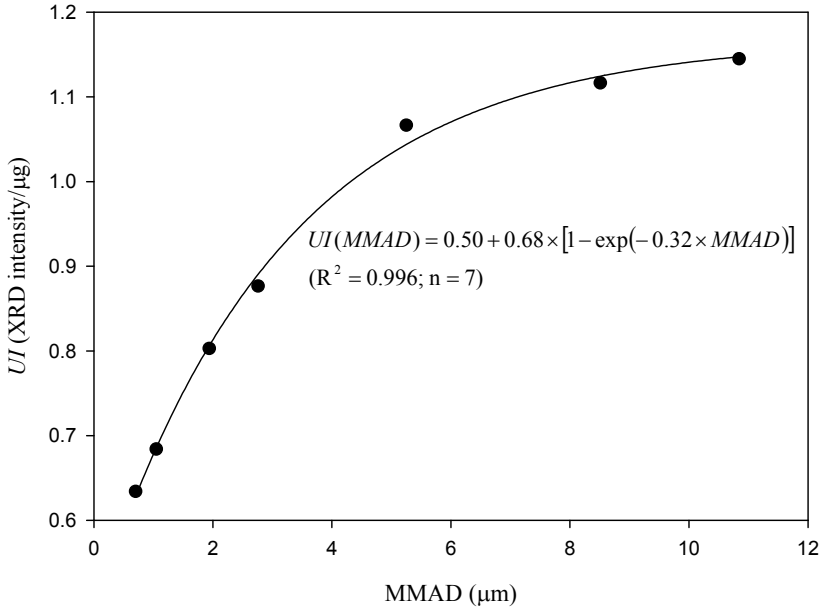

Fig. 3. The relationship between unit intensity (UI) and MMAD of the true quartz particle size.

Table 3. The calculated unit intensities (UI_{ci}) for i^{th} stage Marple cascade impactor and respirable fraction (R_i).

Impaction stage	$d_{ae50\%}$ of Marple cascade impactor (μm)	UI_{ci} (XRD intensity/μg)	R_i
1	21.3	1.18*	0.000
2	14.8	1.17*	0.000
3	9.8	1.15	0.008
4	6	1.08	0.163
5	3.5	0.958	0.624
6	1.55	0.766	0.926
7	0.96	0.680	0.972
8+filter	0.52	0.604	1.000

* Values are extrapolated from Eq. (15).

field sampling site, the XRD intensity (I_i) for sample collected on the i^{th} impaction stage of the cascade impactor was determined per NIOSH Method 7500 (NIOSH, 2003). Therefore, C_{ti}, C_t, C_{mi}, and C_m could be determined by Eq. 4, 5, 8, and 9, respectively, and C_f for converting C_m to C_t could be determined by Eq. (10). In this study, only quartz particle size distributions and their corresponding C_t, C_m, and conversion factors (C_f) were shown in Table 4.

For samples collected from the iron and steel plant, all obtained size distributions were found consistently with a unimodal form (Table 4). Through our field observation, we found that hammering was the main process associated with the generation of aerosols during the stove/oven repairing period. Since hammering could result in brittle fracture of the refractory materials, which has been known as the main mechanism associated with the emission of

Table 4. Particle size distributions of the collected quartz dust samples from seven sampling workplaces/work stages of two sampling plants and their corresponding true quartz concentration (C_t), measured quartz concentrations (C_m), and conversion factors (C_f).

Sampling plant	Sampling workplace/stage	Particle size distributions of the collected quartz dusts (μm) MMAD ± GSD	C_t (mg/m^3)	C_m (mg/m^3)	C_f
Iron and steel plant	Air stove	5.18 ± 2.28	0.242	0.290	0.834
Municipal waste incinerator	Coke oven/Side walk	8.53 ± 2.09	2.95	3.73	0.789
	Coke oven/roof	10.3 ± 2.20	2.33	2.99	0.781
	Stove repairing	15.1 ± 2.71	2.06	2.66	0.775
	Refractory material repairing	16.7 ± 2.08	1.25	1.64	0.765
	Scaffold removing	15.8 ± 2.88	0.410	0.529	0.775
	Stove cleaning	8.50 ± 2.25	25.5	32.2	0.792

coarse dusts with a unimodal form (Zhang *et al.*, 1994; Bianchi *et al.*, 1998; Soo *et al.*, 2011). Therefore, the results obtained from the present study could be theoretically plausible. We also found that MMAD ± GSD obtained from the three selected workplaces of the air stove, coke oven/sidewalk, and coke oven/roof were 5.18 μm ± 2.28, 8.53 μm ± 2.09, and 10.3 μm ± 2.20, respectively (Table 4). Based on our field investigation, we found that both alumina brick and alumina-magnesia brick were used as the refractory material for the workplace of the air stove because of their good heat transfer and storage characteristics. But for the coke oven, both sillimanite brick and silica brick were used as the refractory material for the corrosion and wear prevention purposes. Since the hardness of the involved refractory materials and the hammering strength were not measured in the present study, it might not be possible to explain the differences in particle size distributions among the three selected workplaces. Nevertheless, C_t obtained from the air stove (= 0.242 mg/m^3) was much lower than that from coke oven workplaces (2.95 and 2.33 mg/m^3 for the sidewalk and roof, respectively) (Table 4) which could be partly explained by the fact that both alumina brick and alumina-magnesia brick are known containing less quartz content than that of sillimanite brick and silica brick.

A unimodal particle size distribution of quartz could also be found for samples collected from the four work stages inside a municipal waste incinerator during its annual maintenance period (Table 4). Since the hammering was adopted at both stove repairing, refractory material repairing stages, and hence the emission of coarse dusts with a unimodal form could be possible. Though at the scaffold removing stage no hammering was involved, the aerosols found in the atmosphere could be those generated from the above two work processes but still remained in the workplace atmosphere. As for the stove cleaning stage, the aerosols found in the atmosphere could be mainly due to the re-suspension of aerosols during the floor cleaning process. Therefore, the unimodal form could be explained by the above bulk agitation process. Table 4 also shows MMAD ± GSD of the unimodal quartz particle size distribution for the four selected work stages (= 15.1 μm ± 2.71,16.7 μm ± 2.08, 15.8 μm ± 2.88, and 8.50 μm ± 2.25 for the stove repairing, refractory material repairing, scaffold removing, and stove cleaning, respectively). Here, the particle size of the latter was much finer than that of the former three could be due to the intrinsic differences in the involved aerosol generation mechanisms. On the other hand, the particle sizes of the former three were quite similar indicating that our previous inference could be possible (i.e., sharing the same aerosol generation process or generated aerosols). In this study, C_t for the above four work stages were found as 2.06, 1.25, 0.410, and 25.5 mg/m^3, respectively (Table 4). Since both stove repairing and refractory material repairing involved in the demolition of refractory materials, and hence their concentrations were quite comparable. Because the aerosols found in the scaffold removing process could be mainly coming from those generated from the above two work processes but after sedimentation, it is not surprising to see that its concentration was much lower than that of

the above two work processes. Finally, since the stove cleaning process was used to remove demolished refractory materials, its high concentration might be explained by its high agitation process.

Table 4 also shows C_m, and conversion factors (C_f) for the selected seven workplaces/work stages. It is known that the value of UI is increased as increase in d''_{ae} increased (see Eq. (15)). Since the obtained particle size distributions (MMAD = 5.18–16.7 μm, GSD = 2.08–2.88) were consistently coarser than that of NIST-SRM 1878 (MMAD = 2.16 μm, GSD = 1.55), it is not so surprising to see that all resultant C_m values (= 0.29–32.2 mg/m^3) were higher than their corresponding C_t values (= 0.242–25.535 mg/m^3). As a results, the use of NIST-SRM 1878 as a reference standard for quantification of quartz samples would result in overestimation of field sample concentrations. In the present study, the resultant GSD fell within the range of 2.08–2.88 indicating the variation of the quartz particle size distribution for the seven selected workplaces/work stages were quite similar. In order to properly convert C_m to C_t for samples collected from the field, therefore, a nonlinear regression equation was developed to relate MMAD and its corresponding C_f based on the results obtained from the seven selected workplaces/work stages. This study yielded the regression equation as (Fig. 4):

$$C_f = 0.774 + 0.371 \times [1 - \exp(-0.355 \times \text{MMAD})] \quad (R^2 = 0.980,\ n = 7) \qquad (15)$$

Though particle size distributions obtained from the present study (MMAD = 5.18–16.7 μm, GSD = 2.08–2.88) might cover most particle size distributions which could be encountered in the field, caution should be taken for the use of the above equation if the obtained size distributions fell outside the above designated range.

Respirable Quartz Concentrations and Their Conversion Factors for the Field Collected Samples

In this study, the respirable fraction (R_i) of the i^{th} impaction stages for the cascade impactor used in the present study can be seen in Table 3 based on the criteria currently adopted by the ISO, CEN, and ACGIH (ACGIH, 1995–1996; CEN, 1992; ISO; 1992). By taking R_i into account, CR_{ti}, CR_t, CR_{mi}, CR_m, and CR_f were determined by Eqs. (6), (7), (11), (12), and (13), respectively. In this part of study, only the obtained particle size distributions of the respirable fraction and their corresponding CR_t, CR_m, and CR_f were shown in Table 5.

For all selected workplaces/work stages, the obtained size distributions of the respirable quartz fraction (MMAD = 1.37–1.88 μm, GSD = 2.09–2.87) (Table 5) were finer than that of true total quartz particles (MMAD = 5.18–16.7 μm, GSD = 2.08–2.88) (Table 4). The above results are mainly because the respirable fraction is only a sub-fraction of the true total. But it should be noted that the obtained size distributions of the respirable fraction for the air stove (1.37 μm ± 2.09), stove cleaning (1.80 μm ± 2.87), and coke oven/side walk (1.88 μm ± 2.40) were finer than that of the reference standard of NIST-SRM 1878 (MMAD = 2.16 μm, GSD = 1.55). Therefore, their CR_t (0.062–1.65 mg/m^3) were found to be higher than the corresponding CR_m (0.057–1.63 mg/m^3). As a result, their CR_f (1.01–1.09) were consistently higher than unity. On the other hand, the obtained size distributions of the respirable fraction for the other four workplaces/work stages (MMAD = 2.68–3.95 μm, GSD = 1.97–2.32) were coarser than that of the reference standard of NIST-SRM 1878 (MMAD = 2.16 μm, GSD = 1.55). Therefore, their CR_t (0.035–0.154 mg/m^3) were found to be lower than the corresponding CR_m (0.040–0.166 mg/m^3), and hence the corresponding CR_f (0.866–0.928) were consistently lower than unity.

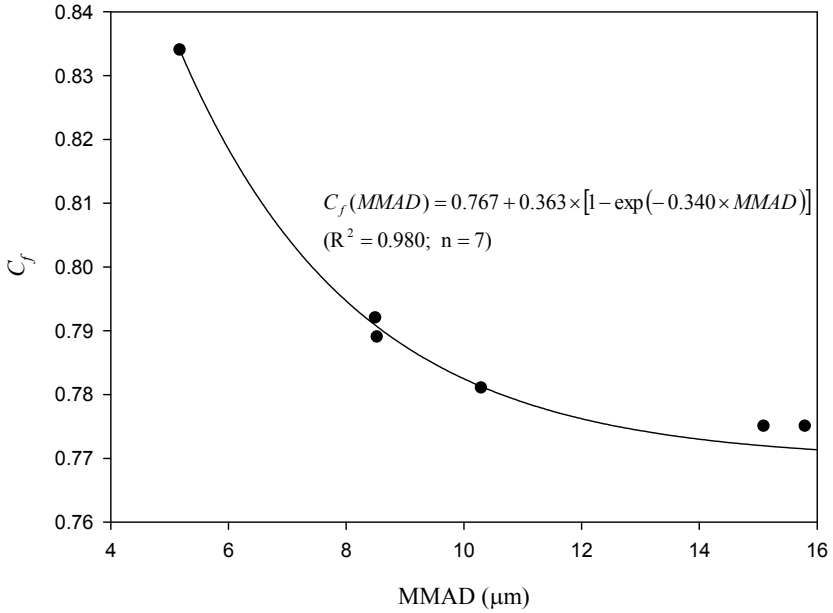

Fig. 4. The relationship between the conversion factors (C_f) and their corresponding MMADs of the true quartz dust for samples collected from the seven selected workplaces/work stages.

Table 5. Particle size distributions of the resprable quartz fraction for samples collected from seven sampling workplaces/work stages of two sampling plants and their corresponding true respirable quartz concentration (CR_t), measured respirable quartz concentrations (CR_m), and conversion factors (CR_f).

Sampling plant	Sampling workplace/stage	Particle size distributions of the respirable fraction of the collected quartz dusts (μm) MMAD ± GSD	CR_t (mg/m^3)	CR_m (mg/m^3)	CR_f
Iron and steel plant	Air stove	1.37 ± 2.09	0.062	0.057	1.09
	Coke oven/Side walk	1.88 ± 2.40	0.190	0.189	1.01
	Coke oven/roof	2.68 ± 1.97	0.154	0.166	0.928
Municipal waste incinerator	Stove repairing	3.60 ± 2.30	0.104	0.118	0.881
	Refractory material repairing	3.95 ± 2.31	0.097	0.112	0.866
	Scaffold removing	3.69 ± 2.32	0.035	0.040	0.875
	Stove cleaning	1.80 ± 2.87	1.65	1.63	1.01

In the present study, we found that all obtained GSDs of the respirable quartz fraction fell within the range of 1.97–2.87 indicating the variations in particle sizes of the collected respirable quartz particle samples from the seven selected workplaces/work stages were quite similar. Therefore, a nonlinear regression equation was developed by relating CR_f to its corresponding MMAD based on the results obtained from the seven collected respirable quartz particle size distributions. This study yielded the regression equation as (Fig. 5):

$$CR_f = 1.50 - 0.67 \times [1 - \exp(-0.69 \times \text{MMAD})] \ (R^2 = 0.996, n = 7) \quad (16)$$

In principle, particle size distributions of the respirable fraction obtained from the present study (MMAD = 1.37–3.95 μm, GSD = 1.97–2.87) would cover most of which could be encountered in the field. However, the use of the above equation for converting CR_m to CR_t in the field should be taken with caution if the obtained size distributions fell outside the above designated range.

CONCLUSION

In this study, we found that quite mono-dispersed pure quartz dusts can be obtained using the liquid sedimentation device developed by the present study. The developed nonlinear regression equation suggests that the value of UI is increased as the increase in MMAD of the separated pure quartz dust. According to field sampling results, the obtained dimensions of the quartz particles in all collected total dust samples were consistently coarser than that of the reference quartz standard. Therefore, all C_m were higher than the corresponding C_t, and all resultant C_f were less than unity. The established nonlinear regression equation of $C_f = 0.774 + 0.371 \times [1 - \exp(-0.355 \times \text{MMAD})]$ would provide a useful basis for converting C_m to C_t for all field collected samples in the future. For the seven field collected respirable dust samples, three and four of them were found with sizes of collected quartz particles finer and coarser than that of NIST-SRM 1878, respectively. Therefore, the CR_t for the former three were higher than the corresponding CR_m, and the resultant CR_f were consistently lower than unity. To the contrary, the latter four were found with CR_t higher than their corresponding CR_m with CR_f consistently higher than unity. This study yielded a regression equation $CR_f = 1.50 - 0.67 \times [1 - \exp(-0.69 \times \text{MMAD})]$ for converting CR_m to CR_t for all collected field samples. However, the obtained converting factors should be the used with caution if collected samples were found with the quartz particle sizes fell outside the size range of the present study.

ACKNOWLEDGEMENT

The authors wish to thank the National Science Council of Taiwan for supporting this research work under Grant NSC NSC98-2221-E-006-023-MY3. The coauthor, C.-Y. Lai, had the same contribution as the corresponding author to this research work.

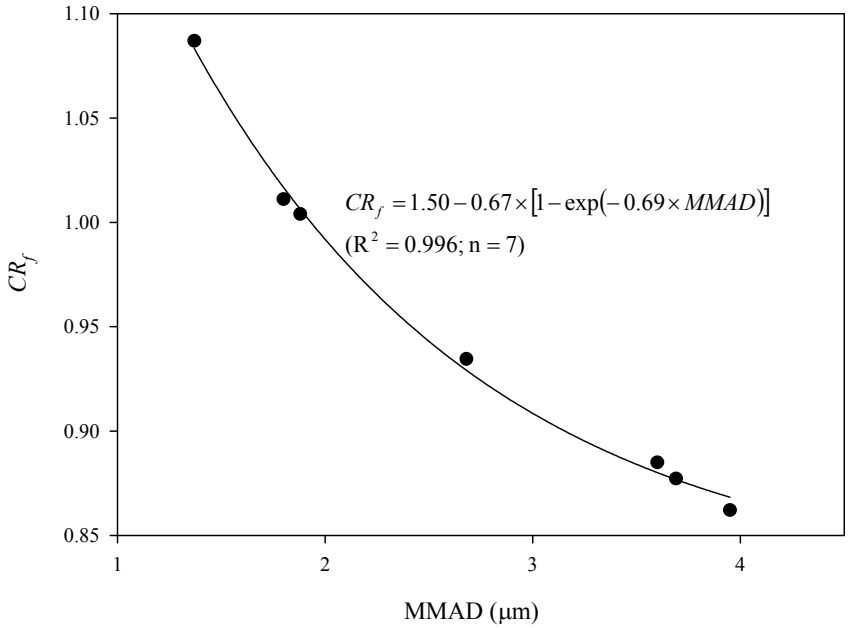

Fig. 5. The relationship between the conversion factors (CR_f) and their corresponding MMADs of the respirable quartz for samples collected from the seven selected workplaces/work stages.

REFERENCES

American Conference of Governmental Industrial Hygienists (ACGIH). (1993–1994). Threshold Limit Values for Chemical Substances and Physical Agents and Biological Exposure Indices, C. Cincinnati, (OH): ACGIH, p. 42–45.

Baron, P.A. and Willeke, K. (2001). Aerosol Measurement: Principles: Techniques, and Applications, Second ed, Wiley, New York Edition, p. 667–701.

Bhaskar, R., Li, J.L. and Xu, L.J. (1994). A Comparative-study of Particle Size Dependency of IR and XRD Methods for Quartz Analysis. *Am. Ind. Hyg. Assoc. J.* 55: 605–609.

Bianchi, E.C., Silva, E.J., Silva, C.E., Souza, G.F., Fortulan, C.A. and Fernandes, O.C. (1998). The Behavior of Resin-bond Diamond Wheels in the Grinding of Advanced Ceramics. *Ind. Diamond Rev.* 58: 105–110.

Chisholm, J. (2005). Comparison of Quartz Standards for X-Ray Diffraction Analysis: HSE A9950 (Sikron F600) and NIST SRM 1878. *Ann. Occup. Hyg.* 49: 351–358.

Comité Européen de Normalization (CEN) (1992). Workplace Atmospheres: Size Fraction Definitions for Measurement of Airborne Particles in the Workplace, CEN, Brussels (Standard EN 481).

Davies, C.N. (1979). Particle Fluid Interaction. *J. Aerosol Sci.* 10: 477–513.

International Standards Organization (ISO) (1992). Air Quality-particle Size Fraction Definitions for Health-related Sampling, International Standards Organization, Geneva (ISO CD7708).

Kauffer, E., Moulut, J.C., Masson, A., Protois, J.C. and Grzebyk, M. (2002). Comparison by X-Ray Diffraction and Infrared Spectroscopy of Two Samples of Alpha Quartz with the NIST SRM 1878a Alpha Quartz. *Ann. Occup. Hyg.* 46: 409–421.

National Institute for Occupational Safety and Health (1994). Silica, Crystalline, by IR, Method 7602 Issue 2 (15/08/94). In NIOSH Manual of Analytical Methods, Cincinnati OH: DHHS (NIOSH).

National Institute for Occupational Safety and Health (2003). Silica, Crystalline, by XRD Method 7500 Issue 4 (15/03/03). In NIOSH Manual of Analytical Methods, Cincinnati OH: DHHS (NIOSH).

Shih, T.S., Lu, P.Y., Chen, C.H., Soo, J.C., Tsai, C.L. and Tsai, P.J. (2008). Exposure Profiles and Source Identifications for Workers Exposed to Crystalline Silica during a Municipal Waste Incinerator Relining Period. *J. Hazard. Mater.* 154: 469–475.

Soo, J.C., Tsai, P.J., Chen, C.H., Chen, M.R., Hsu, H.I. and Wu, T.N. (2011). Influence of Compressive Strength and Applied Force in Concrete on Particles Exposure Concentrations during Cutting Processes. *Sci. Total. Environ.* 409: 3124–3128.

Stacey, P., Kauffer, E., Moulut, J.C., Dion, C., Beauparlant, M., Fernandez, P., Key-Schwartz, R., Friede, B. and Wake, D. (2009). An International Comparison of the Crystallinity of Calibration Materials for the Analysis of Respirable Alpha-quartz Using X-ray Diffraction and a Comparison with Results from the Infrared KBr Disc Method. *Ann. Occup. Hyg.* 53: 639–649.

Verma, D.K. and Shaw, D.S. (2001). A Comparison of International Silica (Alpha-quartz) Calibration Standards by Fourier Transform-Infrared Spectrophotometry. *Ann. Occup. Hyg.* 45: 429–435.

Vincent, J.H. (1995). *Aerosol Science for Industrial Hygienists*, First ed., Elsevier, Pergamon/Elsevier, Oxford, p. 56–62.

Vincent, J.H. (2007). *Aerosol Sampling: Science, Standards*, Instrumentation and Applications, Second ed., John Wiley

and Sons, England, p. 255–287.

William, J.M. (1999). Issues and Controversy: The Measurement of Crystalline Silica; Review Papers on Analytical Methods. *Am. Ind. Hyg. Assoc. J.* 32: 529–553.

Yabuta, J. and Ohta, H. (2003). Determination of Free Silica in Dust Particles: Effect of Particle Size for the X-Ray Diffraction and Phosphoric Acid Methods. *Ind. Health* 41: 249–259.

Zhang, Z., Zhang, L. and Mai, Y. (1994). Modeling Friction and Wear of Scratching Ceramic Particle-reinforced Metal Composites. *Wear* 176: 231–237.

Received for review, April 11, 2013
Accepted, December 25, 2013